Comparison of Meso-Mechanics and Numerical Simulation Based on Particle-Reinforced Composites

Shulei Sun[1*], Wenguo Chen[2]

[1] Department of Mechanics Engineering, Guizhou Institute of Technology, Guiyang 550003, China.
[2] School of Information Engineering, Qujing Normal University, Quijing 655011, China.

* Corresponding author. Tel.: +8617685033619; email: bobsunstuy@gmail.com
Manuscript submitted July 27, 2020; accepted October 11, 2020.
doi: 10.17706/ijapm.2021.11.2.33-42

Abstract: With the macroscopic mechanical properties of the particle reinforced composites, it has been used to approximate theoretical solution for a long time. With the development of computer, the comparison of uniaxial tension and simple shear is performed by the meso-mechanical theory and simulation. The simulation model uses the representative volume element (RVE) with periodic boundary conditions. The macroscopic stress and strain of the volume-averaged method use the Mori-Tanaka model and the Double-Inclusion model based on inclusion theory. The results demonstrate that the results with the meso-mechanics are agreement highly with the numerical simulation in the case of the linear elastic deformation. However, the results with the meso-mechanical method have deviation compared to the numerical simulation in the case of finite deformation.

Keywords: Representative volume element, meso-mechanics, composite materials, numerical simulation, anisotropy.

1. Introduction

Particle-reinforced composites are constituted by adding reinforcement to the matrix material. It has excellent performance so that it is commonly used in aviation, aerospace and automotive fields. A great deal of research work has been undertaken by the meso-mechanical method for its effective performance. Mori and Tanaka [1] predicted the effective elastic properties of particle reinforced composites through the mean-field approximation. The Mori-Tanaka model is deemed to be the simplest model because of its compact form. Based on the Eshelby equivalent inclusion theory, Cheng *et al*. [2] and Sharma *et al*. [3] established a meso-mechanical model containing spherical and elliptical inclusion through extending the Mori-Tanaka method. However, these widely used models do not take into consideration the particles interactions, especially when involved with the high volume ratio of particle-reinforced composites. Meanwhile, the theoretical analysis method can only obtain the macroscopic effective modulus but the details of the local field, and the analysis of specific inclusion details such as the influence of geometric distribution, orientation and shape of the macro modulus. With the development of computers, numerical analysis of composite materials with periodic distribution can be done by establishing a representative volume unit (RVE). For example, Jaensson and Sundstorm [4] used the finite element method to get the elastic modulus and Poisson's ratio of an alloy. Tessier-Doyen *et al*. [5] applied finite element software to simulate the mechanical response of particle-reinforced composites then found that numerical predictions

are very similar to those obtained by Hashin and Shtrikman models [6]. Llorca and Segurado [7] established a modified stochastic continuous absorption algorithm to generate a three-dimensional cube unit cell model with a particle volume fraction up to 50%. A big problem with the numerical simulation is the setting of the volume unit size. Dagan and Willis [8], [9] proved that a small-scale representative volume unit has more accurate prediction results.

For numerical simulation of particle reinforced composite materials using RVE have also been gradually improved, such as Li Qing and Kang Guozheng [10]-[13]. However, there are few references on numerical simulation as well as a comparative study with theoretical solutions in the case of large deformations. For basic works of nonlinear mechanics and composite material mechanics established by Holzapfel A G and Liu hongwen [14], [15].

In general, particles are randomly distributed as well as macroscopically isotropic, if external disturbances, such as a magnetic field, occur, the particles are circulated in a chain along one direction. Thus macroscopically presents itself as transversely isotropic [16]. Galipeau *et al*. [17] studied mechanical responses of the materials in some specific surroundings through building the periodic microstructure of magnetohydro-dynamics. Weng L *et al*. [18] developed a three-dimensional multi-particle finite element model to explore the effects of particle size, morphology and interfacial strength on the elastic-plastic behavior of particle-reinforced composites under uniaxial tension. Xu W *et al.* [19] developed the coupled effects of anisotropic particle geometry and reinforced/weak interphase characteristics (i.e., volume fraction, thickness, moduli and Poisson ratio) on the elastic properties of particle-reinforced composites (PRCs) at nano and microscales. Based on the coupling method of finite element method and smoothed particle hydrodynamics method, the process of single abrasive grain cutting particles reinforced Cu-matrix compo-sites with small volume fraction of particle phase is simulated, and the chip formation mechanism of particle-reinforced Cu-matrix composites was analyzed [20]. Zhang J *et al*. [21] used RVE models containing complex morphology particles to study the effect of particle, matrix and interface damage on the mechanical properties and failure behavior of composites under uniaxial tension. Tian *et al*. [22] proposed a 3D RVE model and forecast the effective elastic parameters of composites by the homogenization method. Xu *et al*. [23] developed full-scale finite element method to study the pseudo-elasticity and shape memory effects of shape memory alloy (SMA) fiber reinforced composites.

2. Particle Reinforced Composite Material Parameters

2.1. Material Parameters

In this paper, the rubber is selected as the matrix material, which can be regarded as a super-elastic materials. Its constitutive model can be derived from the strain energy density function. For the matrix, the Mooney-Rivlin [14] model is used:

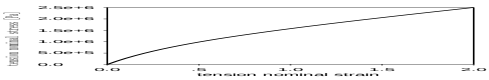

(1)

where, $\bar{I}_1$, $\bar{I}_2$, denote the modified invariants, $\bar{I}_1 = J^{-2/3}I_1$, $\bar{I}_2 = J^{-4/3}I_2$, I_1, I_2 are the first and second invariants for the right Cauchy-Green strain tensor, J is the deformation volume ratios. C_{10}, C_{01} are the two parameters of the matrix. κ is the initial bulk modulus. The shear modulus based on Mooney-Rivlin model is as following:

$$G = 2\left(C_{10} + C_{01}\right) > 0 \tag{2}$$

Here, G is the initial shear modulus. It is assumed that the ratio of: $C_{01} : C_{10}$ is 1:4, then C_{10} is 0.4 MPa,

which C_{20} is 0.1 MPa. The result of G is equal to 1 MPa, then the Poisson's ratio ν is set to 0.47. The bulk modulus [15] can be derived as follow:

$$\kappa = \frac{2G(1+\nu)}{3(1-2\nu)} \tag{3}$$

The bulk modulus $\kappa = 16.33\,\text{MPa}$ can be obtained from the eq. (3).

$$E = 2G(1+\nu) \tag{4}$$

Then the initial Young's modulus E is 2.94MPa.

Fig. 1 is the curve of strain-stress for Mooney-Rivlin matrix under uniaxial tensile. It can be seen from the Fig. 1 that Mooney-Rivlin matrix has nonlinear characteristics under uniaxial tension.

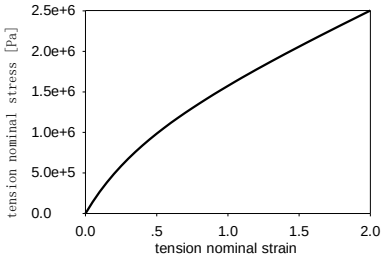

Fig. 1. Uniaxial tension of the Mooney-Rivlin model.

Fig. 2 is the stress-strain curve of simple shear of the matrix under large deformation. It shows that a linear relationship between the nominal stress and the nominal strain in the case of simple shear.

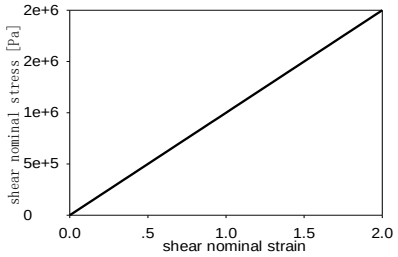

Fig. 2. Shear deformation of the Mooney-Rivlin model.

The filling material of particle reinforced composites are carbonyl iron powder, which is a kind of typical high magnetic permeability, low remanence and high magnetic saturation material. The mechanical parameters of Young's modulus is 210 GPa and Poisson's ratio is 0.33, from the following formula:

$$G = \frac{E}{2(1+\nu)} \tag{5}$$

From the eq.(5), The shear modulus G can be obtained as 78.94 GPa.

2.2. Representative Volume Element

With the development of the computer, the composites can be approached with the real representative volume element by numerical simulation. Even the microstructures can be obtained directly from the CT scans of specimens. However, this method needs a large amount of calculation. The method using a representative volume element does not require the scanning of real materials. Then the macro-effective modulus based on the hypothesis of homogenization will become easy. Fig. 3 is a diagram of the RVE.

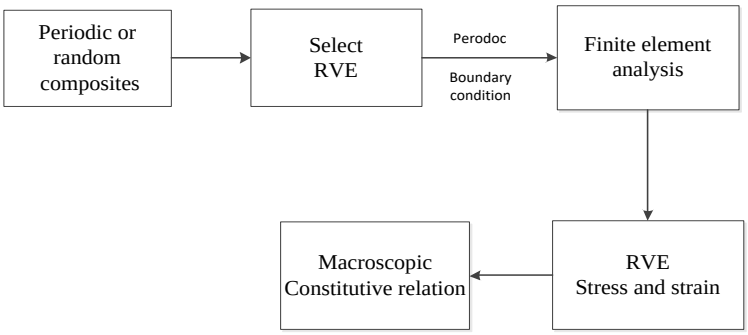

Fig. 3. Diagram of RVE method.

2.3. Size and Establishment of RVE Models

When the particles are separated from the RVE, the part of the particles of the RVE is retained, while the outside of the RVE should be transplanted to the corresponding boundary so that it becomes a complete particle of the RVE. It is set to ensure the continuity of the particles at the boundary as well as to get the repeatability of RVE. Fig. 4 and Fig. 5 are the RVE diagrams in the two-dimensional and three-dimensional cases, respectively. We can find that the particles of the boundary maintain the geometric continuity. For a periodic distribution or a regular array, the definition of the RVE supposes to be a unit element with the periodic characteristics. One parallelogram periodic representative flat element or hexagonal periodic representative volume element can usually be selected for a two-dimensional periodic microstructure, but in numerical simulation, the parallelogram makes the application of periodic boundary conditions become relatively easy. For the periodic structure, the usual method is as follows: select a point in the periodic structure, its surroundings must have its equivalent point, that is, the situation around the two points is exactly the same. Different equivalent points in the two directions are chosen for one point. Periodic representative element can be quickly constructed by this method.

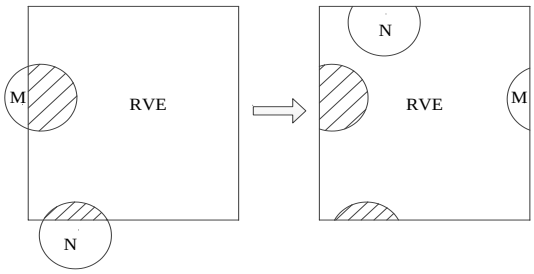

Fig. 4. Plane sketch of geometric model.

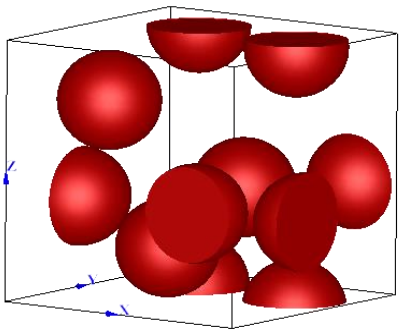

Fig. 5. 3-D sketch of RVE model.

The periodic volume unit can be used to construct the RVE directly. The generation of random inclusion depends on a random algorithm which generates a sphere center as well as inclusion. Once appearing inclusion interference then randomly generate ones in another position. Because this article mainly studies the generation of spherical inclusions, we only pay attention to the random distribution of inclusion instead of inclusion orientation thus ensuring the material isotropic.

As to the selection of the RVE size for the random structure in this paper by comparison with the mechanical properties of different RVE sizes. Finally, a random isotropic RVE with a volume ratio of 0.3 and 30 particles is established. The size of the RVE side length is 3.0×10^{-5} meter.

2.4. Periodical Boundary Conditions

In order to get the equivalent mechanical properties of composites, it is necessary to apply the load and periodic boundary conditions for the RVE. If the RVE is so large that the result is insensitive to any boundary conditions. For the sake of simplicity, there are two loading methods: the one is a rectangular RVE applied to the positioning shift value deforms to another rectangle. Under this loading condition, the stiffness obtained is larger than the actual result according to the principle of minimum potential energy. The other loading method is the stress boundary condition, which the stress condition is imposed on the boundary with application of the principle of minimum residual energy, the predicted rigidity is smaller than reality. These loading methods may be correct when the meso-structure and load of the composites have some symmetry, while in most cases it is just an approximate result with nuances at the boundary. It is not clear boundary effects for large RVE which involved the deviation within the allowable range. For periodic RVE applied to composites with periodic microstructures, periodic boundary conditions should be applied. When composites is uniformly deformed macroscopically, its meso-structure periodic microstructure presents a periodical meso-deformation thus ensuring that the space is seamlessly filled without overlapping. As shown in Fig. 6, the deformation of the opposite edges is coordinated to guarantee the coordination of the deformation field:

(1) Because of the continuous of displacement, the deformation in the adjacent RVE is consistent.

(2) The stress is continuous, which the stress at the corresponding boundary of RVE is consistent.

Assume the corresponding node Q_1 and Q_2 of the opposite edge. The reference coordinates of the Q_1 and Q_2 is $X(Q_1)$ and $X(Q_2)$, respectively. We can obtain the eq. (6):

$$\begin{aligned} \boldsymbol{x}(Q_1) &= \bar{\boldsymbol{F}}\boldsymbol{X}(Q_1) \\ \boldsymbol{x}(Q_2) &= \bar{\boldsymbol{F}}\boldsymbol{X}(Q_2) \end{aligned} \tag{6}$$

When the RVE is deformed, the Q_1 and Q_2 satisfied the displacement relationship:

$$\begin{aligned} \boldsymbol{u}(Q_1) &= \boldsymbol{x}(Q_1) - \boldsymbol{X}(Q_1) = \left(\bar{\boldsymbol{F}} - \mathrm{I}\right)\boldsymbol{X}(Q_1) \\ \boldsymbol{u}(Q_2) &= \boldsymbol{x}(Q_2) - \boldsymbol{X}(Q_2) = \left(\bar{\boldsymbol{F}} - \mathrm{I}\right)\boldsymbol{X}(Q_2) \end{aligned} \tag{7}$$

where RVE is the average deformation tensor. We can calculate from the eq. (7):

$$\boldsymbol{u}(Q_1) - \boldsymbol{u}(Q_2) - \left(\bar{\boldsymbol{F}} - \mathrm{I}\right)\left[\boldsymbol{X}(Q_1) - \boldsymbol{X}(Q_2)\right] = 0 \tag{8}$$

Take a three-dimensional RVE model as an example, as shown in Fig. 7. When the periodic boundary conditions imposed on RVE. The $\mathrm{S_i}$ is the surface boundary and $\mathrm{M_j}$ is the vertex of RVE. According to the requirements of the eqs.(6) and (7), the boundary condition displacement for the 3-D RVE is:

$$\boldsymbol{u}_{\mathrm{S}_4} = \boldsymbol{u}_{\mathrm{S}_3} + \left(\boldsymbol{u}_{M_2} - \boldsymbol{u}_{\mathrm{M}_0}\right) \tag{9}$$

$$\boldsymbol{u}_{S_4} = \boldsymbol{u}_{S_3} + \left(\boldsymbol{u}_{M_2} - \boldsymbol{u}_{M_0}\right) \tag{10}$$

$$\boldsymbol{u}_{S_6} = \boldsymbol{u}_{S_5} + \left(\boldsymbol{u}_{M_3} - \boldsymbol{u}_{M_0}\right) \tag{11}$$

Periodic boundary conditions of stress are

$$\boldsymbol{\sigma}_{S_1} \bullet \boldsymbol{n}_{S_1} = -\boldsymbol{\sigma}_{S_2} \bullet \boldsymbol{n}_{S_2} \tag{12}$$

$$\boldsymbol{\sigma}_{S_3} \bullet \boldsymbol{n}_{S_3} = -\boldsymbol{\sigma}_{S_4} \bullet \boldsymbol{n}_{S_4} \tag{13}$$

$$\boldsymbol{\sigma}_{S_5} \bullet \boldsymbol{n}_{S_5} = -\boldsymbol{\sigma}_{S_6} \bullet \boldsymbol{n}_{S_6} \tag{14}$$

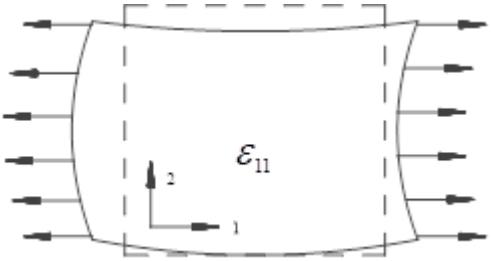

Fig. 6. Sketch of deformation under periodic boundary condition.

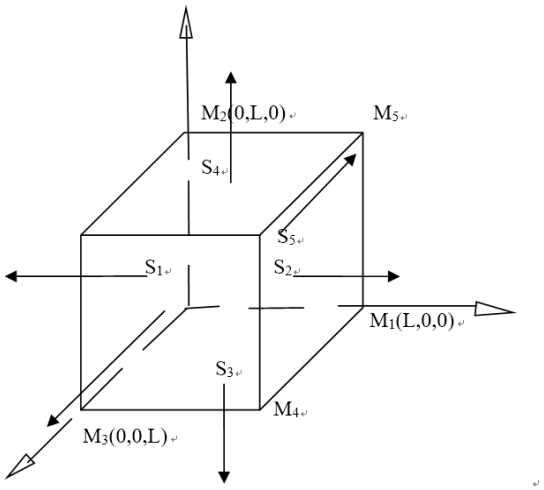

Fig. 7. 3-D sketch of deformation under periodic boundary condition.

3. Comparative Study between Theoretical Solutions and Numerical Simulation in the Case of Uniaxial Tension

Fig. 8 is a periodic geometrical view of an isotropic with a volume ratio of particles of 0.3. Fig. 9 is the deformation of an isotropic elastomer in the case of uniaxial tension. It can be seen that the deformation of the RVE on the surface is so consistent that it satisfies the requirements of the periodic boundary conditions for consistent displacement. The results of numerical simulations of Fig. 10 show that in the case of small deformations, the results are in highly consistent with the results of Mori-Tanaka and Double-Inclusion models, but under large deformations, the deviation between the results of Mori-Tanaka and Double-Inclusion models and those of numerical simulations gradually increases.

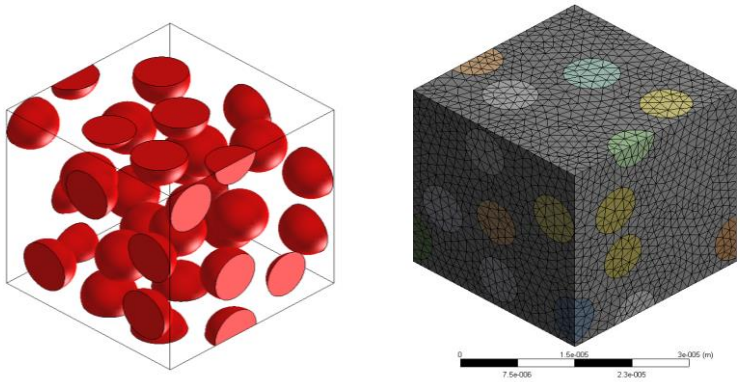

Fig. 8. Schematic diagram of periodic mesh.

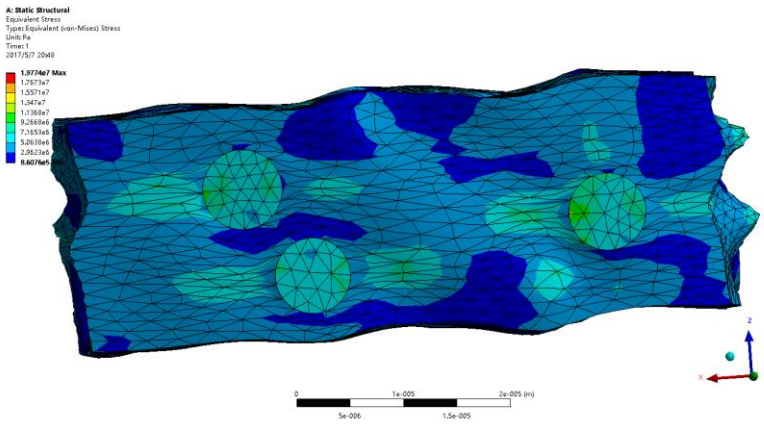

Fig. 9. Uniaxial tension deformation of isotropic MREs.

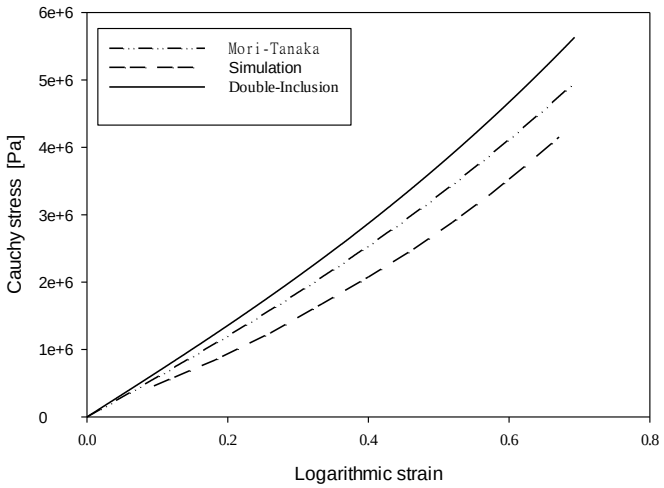

Fig. 10. Uniaxial tension deformation of isotropic MREs.

4. Comparative Study between Simple Shear Numerical Simulation and Theoretical Solution in the Case of Simple Shear

Fig. 11 is the deformation of simple shear. It demonstrates that the boundary deformation of surface is consistent with the application of periodic boundary conditions, which ensuring the reliability of the RVE. Fig. 12 is a diagram of macroscopic stress and strain, which illustrate that for the shear deformation, even if the deformation is small, the results of the Mori-Tanaka model and the Double-Inclusion model are different

from those of the numerical simulation. As the same to stretch, the results of the Mori-Tanaka model and the Double-Inclusion model are higher than the numerical simulation in the case of large deformation.

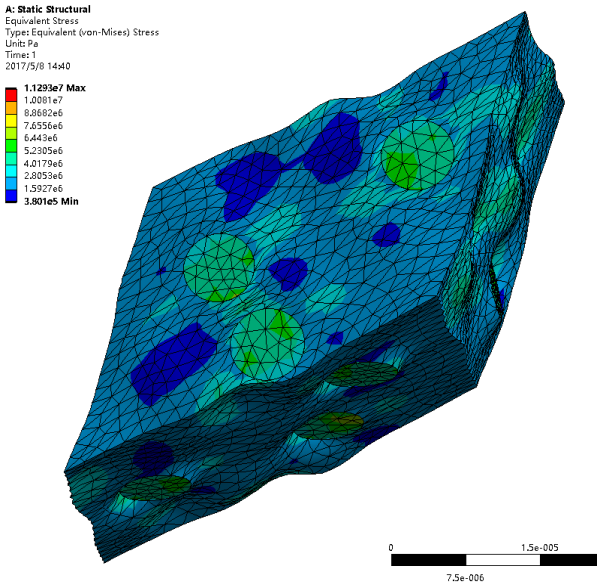

Fig. 11. Simple shear deformation diagrams of isotropic MREs.

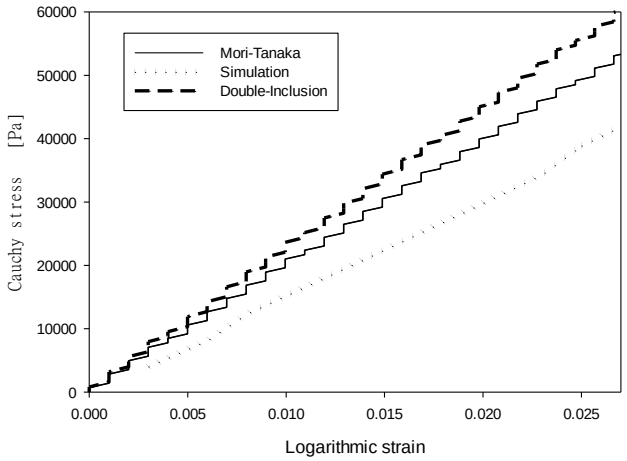

Fig. 12. Simple shear stress and strain curves of isotropic MREs.

5. Conclusion

The representative volume element (RVE) with periodic boundary conditions is used to perform a simulation of uniaxial tension and simple shear. The results of simulation and the theoretical calculation use the Mori-Tanaka model and the Double-Inclusion model show that in the linear elastic deformation the theoretical results are highly consistent with the numerical simulation. However, compared with the numerical simulation under finite deformation, the results use the theoretical calculation with Mori-Tanaka model and the Double-Inclusion model are deviated.

Conflict of Interest

The authors declare that they have no conflicts of interest.

Author Contributions

SLS and WGC conceived and designed the study. SLS performed the simulation. SLS and WGC wrote the

paper. SLS and WGC reviewed and edited the manuscript. All authors read and approved the manuscript.

Acknowledgment

This work was supported by the Joint Foundation of Guizhou Province [2016]7105) and the Nature Science Foundation of Guizhou Province [2016]1063).

References

[1] Mori, T., & Tanaka, K. (1973). Average stress in matrix and average elastic energy of materials with misfitting inclusions. *Acta Metallurgica, 21(5)*, 571-574.

[2] Cheng, Z.-Q., & He, L.-H. (1995). Micropolar elastic fields due to a spherical inclusion. *International Journal of Engineering Science, 33(3)*, 389-397.

[3] Sharma, P., & Dasgupta, A. (2002). Average elastic fields and scale-dependent overall properties of heterogeneous micropolar materials containing spherical and cylindrical inhomogeneities. *Physical Review B, 66(22)*, 224110.

[4] Jaensson, B. O., & Sundstro. B. (1972). Determination of youngs modulus and poissons ratio for Wc-Co alloys by finite element method. *Materials Science and Engineering, 9(4)*, 217.

[5] Tessier-Doyen, N., Glandus, J. C., & Huger, M. (2007). Experimental and numerical study of elastic behavior of heterogeneous model materials with spherical inclusions. *Journal of Materials Science, 42(14)*, 5826-5834.

[6] Hashin, Z., & Shtrikman, S. (1963). A variational approach to the theory of the elastic behaviour of multiphase materials. *Journal of the Mechanics and Physics of Solids, 11(2)*, 127-140.

[7] Segurado, J., & Llorca, J. (2002). A numerical approximation to the elastic properties of sphere-reinforced composites. *Journal of the Mechanics and Physics of Solids, 50(10)*, 2107-2121.

[8] Drugan, W. J., & Willis, J. R. (1996). A micromechanics-based nonlocal constitutive equation and estimates of representative volume element size for elastic composites. *Journal of the Mechanics and Physics of Solids, 44(4)*, 497-524.

[9] Drugan, W. J. (2000). Micromechanics-based variational estimates for a higher-order nonlocal constitutive equation and optimal choice of effective moduli for elastic composites. *Journal of the Mechanics and Physics of Solids, 48(6-7)*, 1359-1387.

[10] Li, Q., & Yang, X. (2012). Numerical analysis on interface instability of cylindrical and spherical shells under implosive loading. *Chinese Journal of Applied Mechanics, (05)*, 607-633.

[11] Jiao, W. (2011). Numerical simulation for ratcheting of particle reined metal matrix composites based on periodical boundary condition. Southwest Jiaotong University.

[12] Guo, S. (2012). Meso-mechanical cyclic constitutive study for the rechetting of particulate reinforced metal matrix composites. Southwest Jiaotong University.

[13] Guo, S. (2009). Finite element analysis for racheting of particle reinforced metal matrix composites. Southwest Jiaotong University.

[14] Holzapfel, A. G. (2000). *Nonlinear Solid Mechanics II*.

[15] Liu, H., & Lin, J. (1997). *Concise Mechanics of Materials*. Higher education press.

[16] Danas, K., Kankanala, S. V., & Triantafyllidis, N. (2012). Experiments and modeling of iron-particle-filled magnetorheological elastomers. *Journal of the Mechanics and Physics of Solids, 60*, 12038.

[17] Galipeau, E., Rudykh, S., Botton, G., & Castaneda, P. P. (2014). Magnetoactive elastomers with periodic and random microstructures. *International Journal of Solids and Structures, 51*, 3012-3024.

[18] Weng, L., Fan, T., Wen, M., *et al*. (2019). Three-dimensional multi-particle FE model and effects of interface damage, particle size and morphology on tensile behavior of particle reinforced composites.

Composite Structures, 209, 590-605.

[19] Xu, W., Wu, Y., & Jia, M. (2018). Elastic dependence of particle-reinforced composites on anisotropic particle geometries and reinforced/weak interphase microstructures at nano-and micro-scales. *Composite Structures, 203*, 124-131.

[20] Su, C., Mi, X., Sun, X., *et al*. (2018). Simulation study on chip formation mechanism in grinding particle reinforced Cu-matrix composites. *International Journal of Advanced Manufacturing Technology, 99(5-8)*, 1249-1256.

[21] Zhang, J., Ouyang, Q., Guo, Q., Li, Z., Fan, G., Su, Y., *et al*. (2016). 3D microstructure-based finite element modeling of deformation and fracture of SiCp/Al composites. *Compos. Sci. Technol., 123*, 1–9.

[22] Tian, W., Qi, L., Su, C., Zhou, J., & Jing, Z. (2016). Numerical simulation on elastic properties of short-fiber-reinforced metal matrix composites: Effect of fiber orientation. *Compos. Struct., 152*,408–417.

[23] Xu, R., Bouby, C., Zahrouni, H., Zineb, T., Hu, H., & Potier-Ferry, M. (2018). 3D modeling of shape memory alloy fiber reinforced composites by multiscale finite element method. *Compos Struct, 200*, 408–419.

Shulei Sun was born in Jingmen, China. He received his Ph.D. from Northwestern Polytechnical University, China, in 2015. Now he is an associate professor of Guizhou Institute of Technology. Guizhou 550003. His fields of interest are solid mechanics and computational mechanics.

Wenguo Chen was born in Qujing, China. He received the B.Sc. and the M.Sc. degrees in Kunming University of Science and Technology, Kunming, China, in 2008 and 2011, respectively. He received the Ph.D. degree in microelectronics and solid state electronics from Shanghai Jiao Tong University, Shanghai, China, in 2015. Now he is an associate professor of College of Information Engineering, Qujing Normal University, Qujing, Yunnan 655000, China. His research interests include the design, simulation and fabrication of MEMS/NEMS devices.